Binding and Reduction of Sulfite by Cytochrome *c* Nitrite Reductase[†,‡]

Peer Lukat,[§] Marc Rudolf,[∥] Petra Stach,[∥] Albrecht Messerschmidt,[⊥] Peter M. H. Kroneck,[∥] Jörg Simon,*[,#] and Oliver Einsle*[,§]

Institut für Mikrobiologie und Genetik, Abteilung Molekulare Strukturbiologie, Georg-August-Universität Göttingen, 37077 Göttingen, Germany, Universität Konstanz, Fachbereich Biologie, 78457 Konstanz, Germany, Max-Planck-Institut für Biochemie, Abteilung Proteomik und Signaltransduktion, 82152 Martinsried, Germany, and Institut für Molekulare Biowissenschaften, Johann Wolfgang Goethe-Universität Frankfurt, 60438 Frankfurt/Main, Germany

Received October 24, 2007; Revised Manuscript Received December 14, 2007

ABSTRACT: Pentaheme cytochrome *c* nitrite reductase (ccNiR) catalyzes the six-electron reduction of nitrite to ammonia as the final step in the dissimilatory pathway of nitrate ammonification. It has also been shown to reduce sulfite to sulfide, thus forming the only known link between the biogeochemical cycles of nitrogen and of sulfur. We have found the sulfite reductase activity of ccNiR from *Wolinella succinogenes* to be significantly smaller than its nitrite reductase activity but still several times higher than the one described for dissimilatory, siroheme-containing sulfite reductases. To compare the sulfite reductase activity of ccNiR with our previous data on nitrite reduction, we determined the binding mode of sulfite to the catalytic heme center of ccNiR from *W. succinogenes* at a resolution of 1.7 Å. Sulfite and nitrite both provide a pair of electrons to form the coordinative bond to the Fe(III) active site of the enzyme, and the oxygen atoms of sulfite are found to interact with the three active site protein residues conserved within the enzyme family. Furthermore, we have characterized the active site variant Y218F of ccNiR that exhibited an almost complete loss of nitrite reductase activity, while sulfite reduction remained unaffected. These data provide a first direct insight into the role of the first sphere of protein ligands at the active site in ccNiR catalysis.

In the metabolic pathway of dissimilatory nitrate ammonification, nitrogen is converted from its most oxidized form, nitrate (NO_3^-), to its fully reduced state, ammonia (NH_3). This reduction by eight electrons is achieved in only two consecutive enzymatic reactions: nitrate reductase produces nitrite (NO_2^-) in a two-electron reduction, which then is reduced to ammonia in a six-electron step by cytochrome *c* nitrite reductase (ccNiR,[1] the NrfA gene product) (*1*, *2*) (eq 1)

$$NO_2^- + 6e^- + 8H^+ \leftrightarrows NH_4^+ + 2H_2O \qquad (1)$$

ccNiR is found in two contexts in different organisms, either in a soluble, periplasmic form such as in *Escherichia coli* or as a membrane-associated complex with a 20 kDa tetraheme cytochrome *c* (NrfH) belonging to the NapC/NirT family of quinol dehydrogenases that serves as an electron donor to the catalytic subunit (*2*−*5*). Being a dissimilatory pathway, nitrite ammonification is coupled to the generation of a proton motive force (pmf) across the cytoplasmic membrane. Using formate or hydrogen as the electron donor, pmf generation is achieved by the redox loop mechanism of either the membrane-bound formate dehydrogenase or the hydrogenase complexes, balanced by electroneutral quinol oxidation by nitrite catalyzed by ccNiR (*2*, *3*, *6*, *7*).

ccNiR is a pentaheme *c*-type cytochrome, the product of the *nrfA* gene (nitrite reduction with formate). Its three-dimensional structure shows the characteristically close packing of heme cofactors into parallel and perpendicular motifs, the exact significance of which is not yet fully understood (*8*, *9*). The active site is formed by heme 1, the single non-bis-histidinyl-coordinated cofactor in the protein. In most known homologues of ccNiR, lysine replaces the canonical histidine residue as the proximal axial ligand of this heme, with the distal axial position providing the site for substrate binding and reduction (*8*). Crystal structures have been presented for ccNiR from *Sulfurospirillum deleyianum* (*10*), *Wolinella succinogenes* (*11*), *E. coli* (*12*), *Desulfovibrio desulfuricans* ATCC 27774 (*13*), and *Desulfovibrio vulgaris* Hildenborough (*5*), and a reaction mechanism has been proposed, based on the observation of substrate and reaction intermediates bound to the *W. succinogenes* enzyme and DFT calculations (*14*). Three conserved amino acid residues are placed around the substrate binding site at heme 1: arginine (R114 in *W. succinogenes*), tyrosine (Y218), and histidine (H277).

[†] This work was supported by the Deutsche Forschungsgemeinschaft (IRTG 1422 to P.L. and O.E., Grant Ei-520/2 to O.E., SFB 472 (P33) to J.S., and SPP 1070 to P.M.H.K.), Volkswagen Stiftung (P.M.H.K.), and the Fonds der Chemischen Industrie (P.M.H.K.).

[‡] Structural data have been deposited in the Protein Data Bank (PDB accession codes 3BNF, 3BNG, 3BNH, and 3BNJ).

* Corresponding authors. (J.S.) Tel.: +49 (69) 798 29516; fax: +49 (69) 798 29527; e-mail: j.simon@bio.uni-frankfurt.de. (O.E.) Tel.: +49 (551) 391 4189; fax: +49 (551) 391 4082; e-mail: oeinsle@uni-goettingen.de.

[§] Georg-August-Universität Göttingen.

[∥] Universität Konstanz.

[⊥] Max-Planck-Institut für Biochemie.

[#] Johann Wolfgang Goethe-Universität Frankfurt.

[1] Abbreviations: NiR, nitrite reductase; SiR, sulfite reductase; ccNiR, cytochrome *c* nitrite reductase.

10.1021/bi7021415 CCC: $40.75
Published on Web 01/18/2008

Prior to the availability of crystal structures, the six-electron reduction of sulfite to sulfide has been reported as a secondary activity of ccNiR for *D. desulfuricans* ATCC 27774 (2.06 μmol of H_2 min^{-1} mg^{-1} in a manometric assay) (*15*) and *S. deleyianum* (1.1 μmol of H_2 min^{-1} mg^{-1}) (*16*) (eq 2)

$$SO_3^{2-} + 6e^- + 7H^+ \leftrightharpoons HS^- + 3H_2O \qquad (2)$$

While significantly lower than the specific activities for nitrite reduction (up to 1050 μmol of NO_2^- min^{-1} mg^{-1} for *S. deleyianum* (*17*), 453 μmol of NO_2^- min^{-1} mg^{-1} for *D. desulfuricans* ATCC 27774 (*18*), and 872 μmol of NO_2^- min^{-1} mg^{-1} for *E. coli* (*12*)), these sulfite reductase activities exceed the ones found for the dissimilatory, siroheme-containing sulfite reductases (*19*), some of which are found in the same organisms as ccNiRs. The conversions of nitrite to ammonia and sulfite to sulfide constitute a remarkable intersection of the biogeochemical cycles of nitrogen and sulfur. Both *S. deleyianum* (*20*) and *W. succinogenes* (*21*) have been shown to grow by oxidation of sulfide to sulfur with fumarate as an electron acceptor, although only *S. deleyianum* was also found to couple the lithotrophic oxidation of sulfide to respiratory nitrate ammonification (*22*). In contrast, nitrate dissimilation was repressed in *W. succinogenes* in the presence of elemental sulfur (*23*) or polysulfide, which is reduced by the membrane-bound polysulfide reductase complex (*24*). While *W. succinogenes* does not grow by the reduction of sulfite, its genome sequence indicated the presence of the protein machinery required for assimilatory sulfate reduction as a means of obtaining sulfur for biosynthetic purposes (*25*). Moreover, *D. vulgaris* Hildenborough, whose NrfHA complex is the only one structurally characterized to date (*5*), was shown not to grow by dissimilatory nitrate reduction (*18*). Its NrfHA complex has instead been suggested to play a role in nitrite detoxification, as nitrate has been shown to inhibit the growth of sulfate-reducing bacteria by the accumulation of toxic nitrite, and the expression of NrfHA can alleviate this effect (*26*). The ability to convert both nitrite and sulfite to their respective, fully reduced forms has also been found for the assimilatory sulfite and nitrite reductases, both of which are cytoplasmic, siroheme-dependent enzymes (*27*−*29*). Nevertheless, a functional role for the periplasmic ccNiR in dissimilatory sulfate reduction remains doubtful, as sulfite is produced from sulfate in the cytoplasm (*26*). However, for enteric bacteria such as *E. coli*—but also *W. succinogenes*—the *nrf* genes have been suggested to function in the detoxification of NO that is produced as a defensive measure by the host (*30*).

In the present work, we investigated the interaction of nitrite and sulfite with the wild-type and a Y218F active site variant of *W. succinogenes* ccNiR, confirming the reductive activity toward sulfite for this organism and elucidating the binding mode of sulfite by X-ray crystallography.

EXPERIMENTAL PROCEDURES

Site-Directed Mutagenesis of W. succinogenes nrfA. Strain *W. succinogenes* Y218F was obtained from *W. succinogenes* Δ*nrfAIJ* (*3*) upon integration of a derivative of plasmid pBR-N3 to restore the entire *nrfHAIJ* operon (the genetic strategy was described previously (*31*)). Site-directed mutagenesis

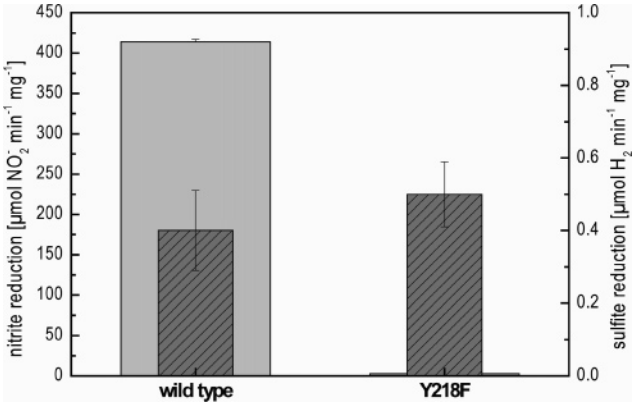

FIGURE 1: Specific activities for the reduction of nitrite (filled) and sulfite (hatched) by *W. succinogenes* ccNiR. Activities are on different scales. Replacement of the active site residue Y218 for phenylalanine drastically reduces nitrite reductase activity but leaves the sulfite reductase activity unchanged within experimental error.

with pBR-N3 as the template was performed using a QuikChange Site-Directed Mutagenesis Kit (Stratagene, La Jolla, CA) and a specifically synthesized primer pair containing the desired mutation (forward primer: 5′-GCCATGTG-GAGT**TT**TACTTCAAAAAGAC-2326). The newly established phenylalanine codon is underlined with the T printed in bold replacing the A of the genuine TAT tyrosine codon. The number at the 3′-end gives the position of the terminal nucleotide in the data bank entry AJ245540. The transformation of *W. succinogenes* Δ*nrfAIJ* with the mutated plasmid was carried out by electroporation as described previously (*32*). Transformants were selected in a medium containing formate and nitrate, kanamycin (25 mg L^{-1}), and chloramphenicol (12.5 mg L^{-1}). The desired integration of the plasmid into the genome via the *nrfH* gene was demonstrated by PCR using suitable primers and DNA from heat-denatured cells as the template.

Analytical Methods. ccNiR was purified in the presence of dioxygen from nitrate-grown cells of *W. succinogenes* following established procedures (*16*, *17*). The protein concentration was determined by the method of Smith et al. using bicinchoninic acid (*33*). Nitrite reductase activity was determined by following the formation of ammonia (*34*). Dithionite-reduced methyl viologen was used as an electron donor for the enzymatic reduction, and ammonia was quantified colorimetrically. The sulfite reductase activity was determined both by monitoring the reoxidation of methyl viologen under anoxic conditions as well as by Warburg manometry according to Steuber et al. (*35*), with Cd(II) acetate in the central compartment of the flask to trap hydrogen sulfide. All assays were performed at least in triplicate, and standard deviations are given in the text and by the error bars in Figure 1.

Structure Determination. Crystals of *W. succinogenes* ccNiR wild-type and Y218F were grown as described previously (*11*) and harvested into a solution containing the reservoir buffer. For the preparation of substrate complexes, 10 mM sodium nitrite or 10 mM sodium sulfite (final concentrations) were added. After incubation for 2 h, 2*R*,3*R*-butane diol was added as a cryoprotectant to a final concentration of 8% (v/v), and the crystals were flash-cooled in liquid nitrogen. Data were collected on beamlines BW7B and X12 of the EMBL outstation at DESY, Hamburg,

Table 1: Data Collection and Refinement Statistics[a]

	NrfA wt SO_3^{2-}	NrfA Y218F native	NrfA Y218F NO_2^-	NrfA Y218F SO_3^{2-}
		Data collection statistics		
PDB code	3BNF	3BNG	3BNH	3BNJ
X-ray source	DESY BW7B	DESY X12	rotating anode	DESY X12
X-ray wavelength (Å)	1.0600	0.9785	1.5418	0.9785
resolution limits (Å)	25.00−1.70	50.00−1.50	30.00−1.75	50.00−1.30
(last shell)	1.79−1.70	1.60−1.50	1.85−1.75	1.39−1.30
no. of unique reflns	73146	108437	69581	161601
Multiplicity	4.6	7.2	7.2	6.9
unit cell dimensions	$a, b = 119.5$ Å	$a, b = 120.0$ Å	$a, b = 120.8$ Å	$a, b = 119.4$ Å
	$c = 186.7$ Å	$c = 186.3$ Å	$c = 186.5$ Å	$c = 184.8$ Å
space group	$I4_122$	$I4_122$	$I4_122$	$I4_122$
completeness (last shell) [%]	98.4 (96.9)	99.4 (97.1)	99.8 (99.2)	98.3 (93.5)
R_{sym} (last shell)	0.069 (0.595)	0.122 (0.663)	0.110 (0.687)	0.114 (0.575)
R_{pim} (last shell)	0.036 (0.304)	0.048 (0.260)	0.043 (0.288)	0.046 (0.250)
I/σ(I) (last shell)	16.4 (2.0)	14.4 (2.7)	12.2 (2.1)	15.3 (2.0)
		Refinement statistics		
R_{cryst}	0.233	0.181	0.184	0.181
R_{free}	0.279	0.215	0.220	0.208
rmsd in bond lengths (Å)	0.019	0.014	0.015	0.011
rmsd in bond angles (deg)	1.778	1.487	1.381	1.326
Cruickshank's DPI (Å)	0.103	0.054	0.074	0.033

[a] Values in parentheses are given for the highest resolution shell. R_{sym} is the residual for symmetry-equivalent reflections according to $R_{sym} = \Sigma_{hkl}(\Sigma_i|I_{hkl(i)} - \langle I_{hkl}\rangle|/\Sigma_{hkl}\Sigma_i I_{hkl(i)})$. R_{pim} is calculated according to Weiss et al. (*44*), and DPI is calculated according to Cruickshank (*45*).

Germany or in-house on a Rigaku MicroMax 007 rotating anode X-ray generator equipped with a mar345dtb image plate system (Table 1). The programs of the HKL suite (*36*) were used for integration and scaling. Phases were obtained from the native structure of *W. succinogenes* ccNiR (PDB code 1FS7) using programs of the CCP4 suite (*37*), and refinement was carried out with REFMAC5 (*38*). All model building was performed with COOT (*39*). Figures were prepared with Molscript (*40*) and Raster3D (*41*) or PyMOL (*42*).

RESULTS

Reactivity of ccNiR with Nitrite and Sulfite. The specific activity for the reduction of nitrite to ammonia was determined to be 414 ± 3 μmol of NO_2^- min^{-1} mg^{-1} for the purified wild-type ccNiR from *W. succinogenes*. For the same protein, the sulfite reductase activity was found to be 0.4 ± 0.11 μmol of H_2 min^{-1} mg^{-1} (Figure 1). Three equivalents of dihydrogen per sulfite were taken up in the manometric assay, in accordance with the stoichiometry (eq 2). Both of these activities are well in the range of activities found for ccNiRs from other organisms. Characteristically, they differ by more than 2 orders of magnitude, indicating a high degree of evolutionary optimization toward the reduction of nitrite. In an earlier study, we proposed a mechanism for the successive transfer of six electrons to nitrite at the active site heme of ccNiR (*14*), and in view of similar electronic properties of the two molecules, an analogous process is expected for the case of sulfite. However, this earlier work did not address the protein residues forming an active site cavity around the distal axial position of heme 1. Changing one of these residues, Tyr 218, to phenylalanine by site-directed mutagenesis resulted in a strong decrease of nitrite reductase activity to 3 ± 1 μmol of NO_2^- min^{-1} mg^{-1}, only 0.7% of the wild-type activity. In contrast, the sulfite reductase activity remained virtually unchanged and was determined to be 0.5 ± 0.09 μmol of H_2 min^{-1} mg^{-1} (Figure 1). The specific activities previously determined by the same method for the dissimilatory, siroheme-dependent sulfite reductases were 0.04−0.1 μmol of H_2 min^{-1} mg^{-1} for the enzyme from *D. desulfuricans* Essex and 0.15−0.3 μmol of H_2 min^{-1} mg^{-1} for *D. vulgaris* Hildenborough sulfite reductase (*19*). While not affecting sulfite reduction, Tyr 218 obviously plays an important role in the reduction of nitrite. To address the effects of the mutation on the binding mode of the substrate, we have therefore determined the three-dimensional structures of complexes with a water molecule, nitrite, and sulfite for both the wild-type and the variant proteins.

Binding of Sulfite to ccNIR. Because of the high activity of ccNiR, it has not been possible to structurally characterize the binding of sulfite to the reduced enzyme. However, as with nitrite, sulfite was bound specifically to the active site of the oxidized enzyme, with the iron atom of heme 1 in the Fe(III) state and the electrons for the coordinative binding being provided by the sulfur atom of the substrate. Only minor changes of the overall structure were observed upon binding of sulfite (Figure 2). The root-mean-squared deviation for all 3450 atom positions of the protein was 0.170 Å between the native structure with a bound water molecule (PDB code 1FS7) and the sulfite complex and 0.168 Å between the sulfite and nitrite adducts (PDB code 2E80). The resolution of the structure obtained with bound sulfite (1.7 Å) was comparable to that of the water and nitrite complexes (1.6 Å). This observed structural rigidity of the protein suggests that the mechanism of nitrite reduction, a multi-electron, multi-proton-transfer process (eq 1), does not require significant structural rearrangements (*14*). Sulfite-soaked crystals clearly showed additional electron density at the substrate binding site, the distal axial position of heme group 1 (Figure 2). This electron density feature could be straightforwardly modeled with a sulfite molecule, coordinated to the heme iron atom through the lone electron pair of its sulfur atom. The oxygen atoms of sulfite were in hydrogen-bonding distance with all immediate active site residues, Arg 114, Tyr 218, and His 277, and a conserved

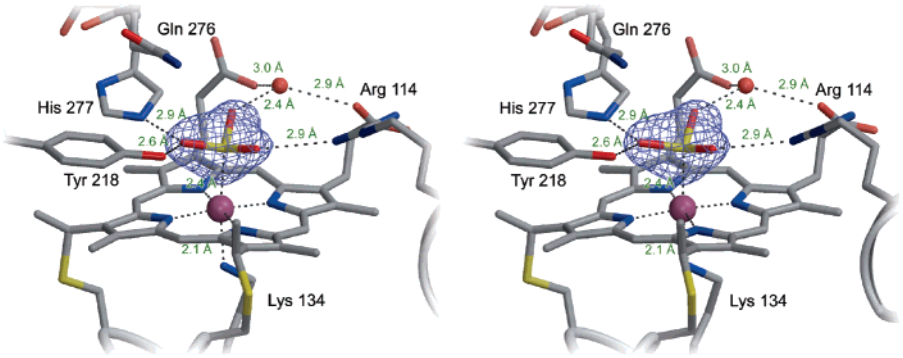

FIGURE 2: Sulfite adduct of *W. succinogenes* ccNiR. A stereo representation of the active site heme group 1, seen in the direction of the substrate entry pathway. The depicted electron density map is a $|F_o| - |F_c|$ difference density map calculated without the sulfite molecule and contoured at a level of 5σ.

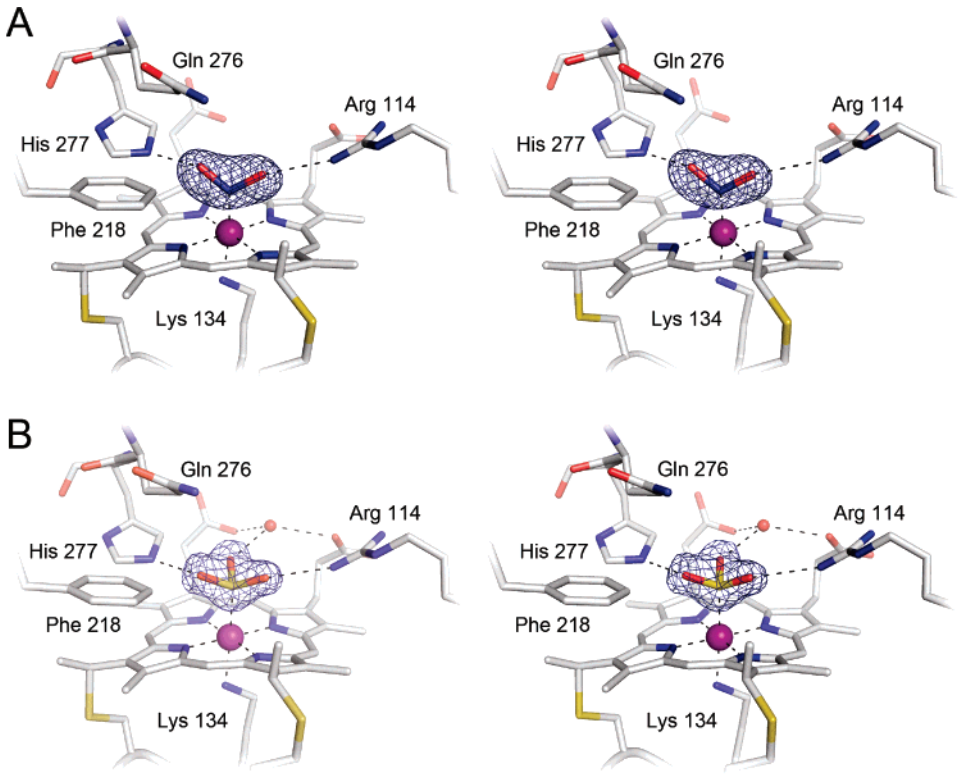

FIGURE 3: Substrate complexes of the Y218F mutant of ccNiR. Stereo representations of the active sites in an orientation as in Figure 2 with the bound substrates nitrite (A) and sulfite (B). The depicted electron density maps are $|F_o| - |F_c|$ difference density maps calculated without the ligand and contoured at a level of 5σ.

water molecule was found to connect the ligand to both propionate side chains of the active site heme group (Figure 2). To form a hydrogen bond to the sulfite ligand, the side chain of Tyr 218 was rotated by ~5° toward its neighbor, His 277. The Fe−S bond distance of 2.4 Å was significantly longer than the Fe−N distance observed in the nitrite adduct (1.9 Å) (*14*), while the bond length and position of the proximal axial ligand, the N_ζ atom of Lys 134, remained unchanged at 2.1 Å.

Substrate Binding to the Y218F Variant of W. succinogenes ccNiR. With only the O_η of Tyr 218 removed, the Y218F variant of ccNiR exhibited minor structural changes as compared to the wild-type enzyme. The benzyl side chain of Phe 218 showed the same ~5° rotation toward His 277 as the wild-type sulfite adduct, and a water molecule that was hydrogen-bonded to Tyr 218 in the wild-type was shifted away from Phe 218 by 0.75 Å. The position of the water molecule bound to the iron atom of heme 1 remained unchanged as did its bond distance of 2.1 Å. A shorter Fe−N bond distance of 1.9 Å was observed in the Fe(III)-nitrite adduct of the wild-type protein (PDB code 2E80), and the same distance was also found in a nitrite complex of the Y218F variant (Figure 3A). The latter again showed the ~5° rotation of the side chain of Phe 218, concomitant with a backward shift of His 277 by 0.4 Å. As a result, the O−N−O plane of the nitrite ligand that was slightly inclined in the wild-type nitrite complex was found to be almost exactly normal to the porphyrin plane of heme 1 (Figure 4A). In both cases, one of the oxygen atoms of nitrite remained perfectly in place, forming a 2.9 Å hydrogen-bonding interaction with the $N_{\eta 2}$ atom of Arg 114, while the other oxygen atom was displaced by 0.6 Å. The hydrogen bond

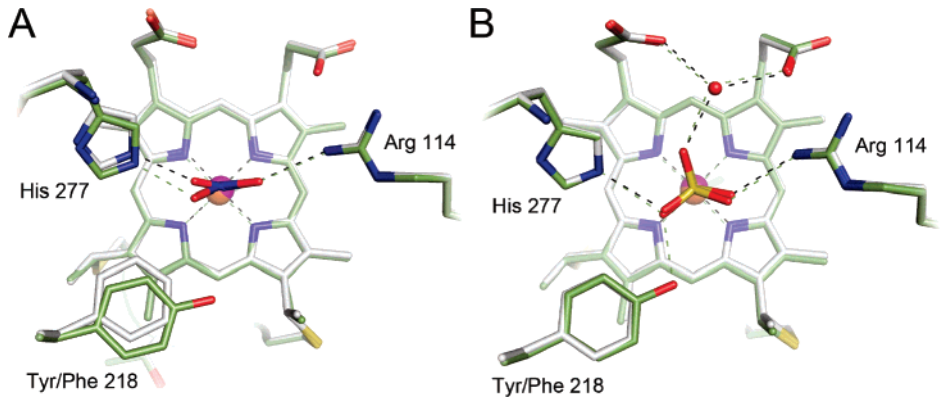

FIGURE 4: Comparison of substrate binding to wild-type and Y218F mutant of ccNiR. (A) In the mutant structure (light gray), Phe 218 is rotated by ~5°, and the nitrite molecule binds in a straighter orientation to His 277 that in turn is shifted backward. The interaction of nitrite with Arg 114 remains unchanged. (B) The binding of sulfite to heme one of ccNiR is practically unaffected by the Y218F mutation, although in the wild-type structure (green), Tyr 218 is in direct hydrogen-bonding contact with the ligand.

formed from this oxygen atom to $N_{\epsilon 2}$ of His 277 was shortened from 2.6 to 2.5 Å. Note that Tyr 218 was not directly involved in hydrogen-bonding interactions with the nitrite molecule in the wild-type enzyme.

The sulfite complex of the Y218F variant yielded crystals diffracting to 1.3 Å resolution, resulting in the most precise three-dimensional structure of a ccNiR available to date (Figure 3B). The sulfite ligand was clearly defined, binding in an identical orientation as in the wild-type. The ~5° rotation of Tyr 218 there was mirrored by Phe 218 in the variant structure, such that both sulfite complexes show the same orientation of the aromatic ring at position 218 and align with an overall root-mean-squared deviation of only 0.26 Å for all protein atoms (Figure 4B).

The hydrophobic roof and the exit channel in the rear part of the active site (*10*, *11*) did not participate in substrate binding, and the water molecules found in the putative product exit channel of the enzyme were found in identical positions in all structures. The first of these water molecules is the one coordinated to both propionate side chains of heme 1. It was present in all structures, but only in the one with bound sulfite did it interact directly with the heme ligand. In the structures without soaked substrates, the heme-ligating water molecules—and in analogy, the two reaction products NH_4^+ and HS^- (eqs 1 and 2)—were too far away from any of the surrounding residues to interact via hydrogen-bond formation. Any such interaction would be likely to stabilize the binding of the products in the active site and would be mechanistically undesirable.

DISCUSSION

Implications of the Y218F Mutation. A most surprising finding was that the exchange of Tyr 218 to Phe drastically reduced the nitrite reductase activity but left the sulfite reductase activity unaltered. While fully conserved in all ccNiR sequences known to date, Tyr 218 does not directly participate in the coordination of nitrite, and so far, there is no evidence for the requirement of a tyrosine radical at any point in the reaction cycle (*14*). Tyr 218 does, however, directly bind to sulfite—whose reduction is not affected by the Y218F mutation—through an H-bond to an oxygen atom. Our crystal structures show that the sulfite complexes of the wild-type and ccNiR variant are virtually identical and that the removal of the O_η of Tyr 218 does not alter the binding mode of the substrate (Figure 4B). In contrast, the substrate nitrite showed a slight rearrangement in the mutant structure, due to a shift of His 277 that was in turn induced by the rotation of the side chain of Phe 218, which was no longer fixed by hydrogen bonding (Figure 4A). It seems unlikely though that this minor structural change alone can account for a drop in activity by 2 orders of magnitude, indicating a more direct involvement of Tyr 218 at some point in the catalytic sequence.

When considering mechanistic implications of the Y218F mutation, note that the assays for nitrite reductase activity are based on the determination of the product ammonia, while the sulfite reductase activity has been assayed colorimetrically by monitoring the oxidation of the redox dye methyl viologen or manometrically by measuring the uptake of dihydrogen. Thus, the NiR assay could not detect the formation of possible reaction intermediates of the conversion of nitrite to ammonia, such as NO, N_2O, or NH_2OH (*14*). It is well-conceivable that the Y218F variant is still able to reduce nitrite at a reasonably high rate but does not carry out the full six-electron reduction to ammonia, such that instead an as yet unidentified intermediate is released. Further studies will be required to clarify this point, and to this end, efficient quantitation methods for the reaction intermediates mentioned previously will have to be established.

Mechanistic Parallels in the Six-Electron Reductions of ccNiR. For the six-electron reduction of nitrite to ammonia, a mechanism has been proposed where a stepwise and alternating transfer of electrons and protons leads to the consecutive release of two waters with the product ammonia remaining bound to the heme iron (*14*). A similar mechanism was proposed for the reduction of sulfite by the assimilatory siroheme-containing sulfite reductase from *E. coli*, where the sulfur atom changes its oxidation state from +IV in SO_3^{2-} to −II in H_2S, without the release of intermediates (*27*, *43*) (eq 2). As in the case of nitrite reduction by ccNiR (*14*), a π back-bonding that transfers charge from the iron atom at heme 1 into a sulfite π^* orbital should be able to stabilize the ccNiR−sulfite complex in the reduced (Fe(II)) state only, facilitating the first S−O bond cleavage. However, due to the longer Fe−S bond and the geometry of the sulfite molecule, which is not in favor of an optimal orbital alignment, this interaction should be less effective than in the case of nitrite. As this π back-bonding interaction will

depend on the respective orientation of the orbitals involved, the slight straightening of the nitrite ligand in the mutant complex may be important. Further DFT calculations for the Y218F variant will help to quantitate this effect.

Another significant difference between the reductions of nitrite and of sulfite lies in the nature of the product. While in the nitrite reductase reaction the anion nitrite is converted to the NH_4^+ cation, the reduction of sulfite leads to H_2S or—depending on local pH—to the HS^- anion (eqs 1 and 2). In the structures of both *S. deleyianum* and *W. succinogenes* ccNiR, a channel has been identified that crosses the entire protein passing the active site (*10*, *11*). This channel has a strongly positive electrostatic surface potential close to the entry to the reactive, distal side of heme 1, but passing it, this surface property changes toward a negative electrostatic potential that leads to a product exit on the opposite side of the enzyme. In case of the conversion of an anion to a cation such as in the reduction of nitrite, this feature allows for a vectorial flow of reaction educts and products and effectively avoids the problem of product inhibition. For sulfite, however, both substrate and product should be anions, and consequently, product inhibition should be an issue.

We have shown that sulfite, as an alternative substrate of ccNiR, binds to the active site in a manner analogous to that of nitrite, and we assume that the reduction of sulfite proceeds along a similar pathway. While the siroheme-containing enzymes underline that the capacity for nitrite and sulfite reduction is likely to be found in the same enzyme, the role of ccNiR in sulfite respiration and in growth on elemental sulfur remains to be clarified.

ACKNOWLEDGMENT

Klaus Sulger and Johannes Larsch are thanked for excellent laboratory assistance. Synchrotron data were collected at the EMBL X12 beamline at the DORIS storage ring, DESY, Hamburg, Germany.

REFERENCES

1. Einsle, O., and Kroneck, P. M. H. (2004) Structural basis of denitrification, *Biol. Chem. 385*, 875−883.
2. Simon, J. (2002) Enzymology and bioenergetics of respiratory nitrite ammonification, *FEMS Microbiol. Rev. 26*, 285−309.
3. Simon, J., Gross, R., Einsle, O., Kroneck, P. M. H., Kröger, A., and Klimmek, O. (2000) A NapC/NirT-type cytochrome *c* (NrfH) is the mediator between the quinone pool and the cytochrome *c* nitrite reductase of *Wolinella succinogenes*, *Mol. Microbiol. 35*, 686−696.
4. Einsle, O., Stach, P., Messerschmidt, A., Klimmek, O., Simon, J., Kröger, A., and Kroneck, P. M. H. (2002) Crystallization and preliminary X-ray analysis of the membrane-bound cytochrome *c* nitrite reductase complex (NrfHA) from *Wolinella succinogenes*, *Acta Crystallogr., Sect. D: Biol. Crystallogr. 58*, 341−342.
5. Rodrigues, M. L., Oliveira, T. F., Pereira, I. A. C., and Archer, M. (2006) X-ray structure of the membrane-bound cytochrome *c* quinol dehydrogenase NrfH reveals novel haem coordination, *EMBO J. 25*, 5951−5960.
6. Cole, J. A. (1990) Physiology, biochemistry, and genetics of nitrate dissimilation to ammonia, in *Denitrification in Soil and Sediments* (Revsbech, N. P., and Sørensen, J., Eds.) pp 57−76, Plenum Press, New York.
7. Cole, J. A., and Brown, C. M. (1980) Nitrite reduction to ammonia by fermentative bacteria: A short circuit in the biological nitrogen cycle, *FEMS Microbiol. Lett. 7*, 65−72.
8. Einsle, O. (2001) Cytochrome *c* nitrite reductase, in *Handbook of Metalloproteins* (Messerschmidt, A., Huber, R., Poulos, T., and Wieghardt, K., Eds.) Wiley and Sons, NewYork.
9. Iverson, T. M., Arciero, D. M., Hsu, B. T., Logan, M. S. P., Hooper, A. B., and Rees, D. C. (1998) Heme packing motifs revealed by the crystal structure of the tetra-heme cytochrome c_{554} from *Nitrosomonas europaea*, *Nat. Struct. Biol. 5*, 1005−1012.
10. Einsle, O., Messerschmidt, A., Stach, P., Bourenkov, G. P., Bartunik, H. D., Huber, R., and Kroneck, P. M. H. (1999) Structure of cytochrome *c* nitrite reductase, *Nature (London, U.K.) 400*, 476−480.
11. Einsle, O., Stach, P., Messerschmidt, A., Simon, J., Kröger, A., Huber, R., and Kroneck, P. M. H. (2000) Cytochrome *c* nitrite reductase from *Wolinella succinogenes*: Structure at 1.6 Å resolution, inhibitor binding, and heme-packing motifs, *J. Biol. Chem. 275*, 39608−39616.
12. Bamford, V. A., Angove, H. C., Seward, H. E., Thomson, A. J., Cole, J. A., Butt, J. N., Hemmings, A. M., and Richardson, D. J. (2002) Structure and spectroscopy of the periplasmic cytochrome *c* nitrite reductase from *Escherichia coli*, *Biochemistry 41*, 2921−2931.
13. Cunha, C. A., Macieira, S., Dias, J. M., Almeida, G., Goncalves, L. L., Costa, C., Lampreia, J., Huber, R., Moura, J. J. G., Moura, I., and Romao, M. J. (2003) Cytochrome *c* nitrite reductase from *Desulfovibrio desulfuricans* ATCC 27774: The relevance of the two calcium sites in the structure of the catalytic subunit (NrfA), *J. Biol. Chem. 278*, 17455−17465.
14. Einsle, O., Messerschmidt, A., Huber, R., Kroneck, P. M. H., and Neese, F. (2002) Mechanism of the six-electron reduction of nitrite to ammonia by cytochrome *c* nitrite reductase, *J. Am. Chem. Soc. 124*, 11737−11745.
15. Pereira, I. A. C., LeGall, J., Xavier, A. V., and Teixeira, M. (2000) Characterization of a heme *c* nitrite reductase from a non-ammonifying microorganism, *Desulfovibrio vulgaris* Hildenborough, *Biochim. Biophys. Acta 1481*, 119−130.
16. Stach, P., Einsle, O., Schumacher, W., Kurun, E., and Kroneck, P. M. H. (2000) Bacterial cytochrome *c* nitrite reductase: New structural and functional aspects, *J. Inorg. Biochem. 79*, 381−385.
17. Schumacher, W., Hole, U., and Kroneck, P. M. H. (1994) Ammonia-forming cytochrome *c* nitrite reductase from *Sulfurospirillum deleyianum* is a tetraheme protein: New aspects of the molecular composition and spectroscopic properties, *Biochem. Biophys. Res. Commun. 205*, 911−916.
18. Pereira, I. C., Abreu, I. A., Xavier, A. V., LeGall, J., and Teixeira, M. (1996) Nitrite reductase from *Desulfovibrio desulfuricans* (ATCC 27774): A heterooligomer heme protein with sulfite reductase activity, *Biochem. Biophys. Res. Commun. 224*, 611−618.
19. Steuber, J., Arendsen, A. F., Hagen, W. R., and Kroneck, P. M. H. (1995) Molecular properties of the dissimilatory sulfite reductase from *Desulfovibrio desulfuricans* (Essex) and comparison with the enzyme from *Desulfovibrio vulgaris* (Hildenborough), *Eur. J. Biochem. 233*, 873−879.
20. Wolfe, R. S., and Pfennig, N. (1977) Reduction of sulfur by spirillum-5175 and syntrophism with *Chlorobium*, *Appl. Environ. Microbiol. 33*, 427−433.
21. Macy, J. M., Schröder, I., Thauer, R. K., and Kröger, A. (1986) Growth of *Wolinella succinogenes* on H_2S plus fumarate and on formate plus sulfur as energy sources, *Arch. Microbiol. 144*, 147−150.
22. Eisenmann, E., Beuerle, J., Sulger, K., Kroneck, P. M. H., and Schumacher, W. (1995) Lithotrophic growth of *Sulfurospirillum deleyianum* with sulfide as electron donor coupled to respiratory reduction of nitrate to ammonia, *Arch. Microbiol. 164*, 180−185.
23. Lorenzen, J. P., Kröger, A., and Unden, G. (1993) Regulation of anaerobic respiratory pathways in *Wolinella succinogenes* by the presence of electron acceptors, *Arch. Microbiol. 159*, 477−483.
24. Hedderich, R., Klimmek, O., Kröger, A., Dirmeier, R., Keller, M., and Stetter, K. O. (1998) Anaerobic respiration with elemental sulfur and with disulfides, *FEMS Microbiol. Rev. 22*, 353−381.
25. Baar, C., Eppinger, M., Raddatz, G., Simon, J., Lanz, C., Klimmek, O., Nandakumar, R., Gross, R., Rosinus, A., Keller, H., Jagtap, P., Linke, B., Meyer, F., Lederer, H., and Schuster, S. C. (2003) Complete genome sequence and analysis of *Wolinella succinogenes*, *Proc. Natl. Acad. Sci. U.S.A. 100*, 11690−11695.
26. Greene, E. A., Hubert, C., Nemati, M., Jenneman, G. E., and Voordouw, G. (2003) Nitrite reductase activity of sulphate-reducing bacteria prevents their inhibition by nitrate-reducing, sulphide-oxidizing bacteria, *Environ. Microbiol. 5*, 607−617.

27. Crane, B. R., Siegel, L. M., and Getzoff, E. D. (1995) Sulfite reductase structure at 1.6 Å: Evolution and catalysis for reduction of inorganic anions, *Science (Washington, DC, U.S.) 270*, 59−67.
28. Swamy, U., Wang, M. T., Tripathy, J. N., Kim, S. K., Hirasawa, M., Knaff, D. B., and Allen, J. P. (2005) Structure of spinach nitrite reductase: Implications for multi-electron reactions by the iron-sulfur:siroheme cofactor, *Biochemistry 44*, 16054−16063.
29. Wolfe, B. M., Lui, S. M., and Cowan, J. A. (1994) Desulfoviridin, a multimeric-dissimilatory sulfite reductase from *Desulfovibrio vulgaris* (Hildenborough): Purification, characterization, kinetics, and EPR studies, *Eur. J. Biochem. 223*, 79−89.
30. Poock, S. R., Leach, E. R., Moir, J. W. B., Cole, J. A., and Richardson, D. J. (2002) Respiratory detoxification of nitric oxide by the cytochrome *c* nitrite reductase of *Escherichia coli*, *J. Biol. Chem. 277*, 23664−23669.
31. Pisa, R., Stein, T., Eichler, R., Gross, R., and Simon, J. (2002) The *nrfI* gene is essential for the attachment of the active site haem group of *Wolinella succinogenes* cytochrome *c* nitrite reductase, *Mol. Microbiol. 43*, 763−770.
32. Simon, J., Gross, R., Ringel, M., Schmidt, E., and Kröger, A. (1998) Deletion and site-directed mutagenesis of the *Wolinella succinogenes* fumarate reductase operon, *Eur. J. Biochem. 251*, 418−426.
33. Smith, P. K., Krohn, R. I., Hermanson, G. T., Mallia, A. K., Gartner, F. H., Provenzano, M. D., Fujimoto, E. K., Goeke, N. M., Olson, B. J., and Klenk, D. C. (1985) Measurement of protein using bicinchoninic acid, *Anal. Biochem. 150*, 76−85.
34. Liu, M.-C., Liu, M.-Y., Payne, W. J., Peck, H. D., Jr., and LeGall, J. (1983) *Wolinella succinogenes* nitrite reductase: Purification and properties, *FEMS Microbiol. Lett. 19*, 201−206.
35. Steuber, J., Cypionka, H., and Kroneck, P. M. H. (1994) Mechanism of dissimilatory sulfite reduction by *Desulfovibrio desulfuricans*: Purification of a membrane-bound sulfite reductase and coupling with cytochrome c_3 and hydrogenase, *Arch. Microbiol. 162*, 255−260.
36. Otwinowski, Z., and Minor, W. (1996) Processing of X-ray diffraction data collected in oscillation mode, *Methods Enzymol. 276*, 307−326.
37. Collaborative Computational Project No. 4. (1994) The CCP4 Suite: Programs for protein crystallography, *Acta Crystallogr., Sect. D: Biol. Crystallogr. 50*, 760−763.
38. Murshudov, G. N., Vagin, A. A., and Dodson, E. J. (1997) Refinement of macromolecular structures by the maximum-likelihood method, *Acta Crystallogr., Sect. D: Biol. Crystallogr. 53*, 240−255.
39. Emsley, P., and Cowtan, K. (2004) Coot: Model-building tools for molecular graphics, *Acta Crystallogr., Sect. D: Biol. Crystallogr. 60*, 2126−2132.
40. Kraulis, P. (1991) MOLSCRIPT: A program to produce both detailed and schematic plots of proteins, *J. Appl. Crystallogr. 24*, 946−950.
41. Merritt, E. A., and Bacon, D. J. (1997) Raster3D: Photorealistic molecular graphics, *Methods Enzymol. 277*, 505−524.
42. Brünger, A. T., Adams, P. D., Clore, G. M., Delano, W. L., Gros, P., Grosse, Kunstleve, R. W., Jiang, J. S., Kuszewski, J., Nilges, M., Pannu, N. S., Read, R. J., Rice, L. M., Simonson, T., and Warren, G. L. (1998) Crystallography and NMR system: A new software suite for macromolecular structure determination, *Acta Crystallogr., Sect. D: Biol. Crystallogr. 54*, 905−921.
43. Crane, B. R., Siegel, L. M., and Getzoff, E. D. (1997) Probing the catalytic mechanism of sulfite reductase by X-ray crystallography: Structures of the *Escherichia coli* hemoprotein in complex with substrates, inhibitors, intermediates, and products, *Biochemistry 36*, 12120−12137.
44. Weiss, M. S. and Hilgenfeld, R. (1997) On the use of the merging R factor as a quality indicator for X-ray data, *J. Appl. Crystallogr. 30*, 203−205.
45. Cruickshank, D. W. J. (1999) Remarks about protein structure precision, *Acta Crystallogr., Sect. D: Biol. Crystallogr. 55*, 583−601.

BI7021415